

2024 年度职称评审论文第一通讯作者认定证明

工号	104097	姓名	卢致文	所在单位	轻纺工程学院
论文题目	Structural deformation dynamic simulation of weft knitted fabric basic stitch				
论文所有作者 (通讯作者用*号标记)	Chenyu Chang, Mingming Song, Feng Liu, Xiaoyan Li, Zhiwen Lu*				
本人是否署名 排名第一的通讯作者	<input checked="" type="checkbox"/> 是 <input type="checkbox"/> 否				
<p>本人申请将此论文作为 <u>2024</u> 年职称评审的有效条件 (第一通讯作者身份发表的学术论文), 承诺所填内容真实有效, 无虚假隐瞒情况。如有问题, 由此引发的一切纠纷及后果由本人承担。</p> <p align="right">本人签名: <u>卢致文</u> 2024年10月18日</p>					
<p>论文所有作者意见: <input checked="" type="checkbox"/>同意 <input type="checkbox"/>不同意 该职称申报人为此论文的第一通讯作者。</p> <p>论文所有作者签名: <u>卢致文 宋明明 刘辉 李燕 卢致文</u></p>					
<p>所在单位认定意见:</p> <p><u>情况属实</u></p> <p align="right">  二级单位负责人 (签字): <u>王</u> (盖章) 2024年10月21日 </p>					
<p>科学技术研究院认定意见:</p> <p align="right">  部门负责人 (签字): <u>王</u> (盖章) 2024年10月21日 </p>					

备注: 本人如为论文的通讯作者应填写此表格, 如为论文的第一作者无须填写。

Structural deformation dynamic simulation of weft knitted fabric basic stitch

Chenyu Chang, Mingming Song, Feng Liu, Xiaoyan Li & Zhiwen Lu

To cite this article: Chenyu Chang, Mingming Song, Feng Liu, Xiaoyan Li & Zhiwen Lu (08 Apr 2024): Structural deformation dynamic simulation of weft knitted fabric basic stitch, The Journal of The Textile Institute, DOI: [10.1080/00405000.2024.2337316](https://doi.org/10.1080/00405000.2024.2337316)

To link to this article: <https://doi.org/10.1080/00405000.2024.2337316>



Published online: 08 Apr 2024.



Submit your article to this journal [↗](#)



Article views: 24



View related articles [↗](#)



View Crossmark data [↗](#)

Structural deformation dynamic simulation of weft knitted fabric basic stitch

Chenyu Chang^a, Mingming Song^a, Feng Liu^a, Xiaoyan Li^b and Zhiwen Lu^{a,b}

^aCollege of Textile Engineering, Taiyuan University of Technology, Jinzhong, China; ^bAnhui Tianzhu Textile Science Technology Co., Ltd, Fuyang, China

ABSTRACT

To address the current problem of separating the structural and deformation models of weft knitted fabrics' basic stitch, and to achieve synchronous simulation of the stitch's structural form and deformation behavior, we studied the structural form and deformation behavior of the basic stitch, including weft plain stitch, rib stitch, and purl stitch. We established a three-dimensional structural model and conducted data analysis, improving the traditional mass-spring model to obtain a deformation model that fits better with the knitted fabric. We then investigated the connection between the structural and deformation models and constructed a correlation model, and used NURBS (Non-Uniform Rational B-Splines) curve application, force analysis, and dynamic solution to study the simulation of the correlation model. Finally, based on computer technology, we achieved dynamic simulation of the structural deformation of weft knitted fabrics' basic stitch and demonstrated the simulation effect, proving the feasibility of the method and the rationality of the model.

ARTICLE HISTORY

Received 30 May 2023
Accepted 26 March 2024

KEYWORDS

Weft knitted fabrics; basic stitch; mass-spring model; correlation model; dynamic simulation

1. Introduction

Weft knitted fabrics can generally be divided into three categories based on the composition elements and complexity of their stitch: basic stitch, patterned stitch, and fancy stitch. Basic stitch, also known as original stitch, form the foundation for all other stitch (de Araújo et al., 2004). Weft Knitted Fabrics are widely utilized due to their diverse structures and comfortable softness. However, their excellent stretch and elastic recovery properties mean they are susceptible to deformation under stress, which can impact product usability and production quality (Frydrych et al., 2018). Research into simulating Weft Knitted Fabrics holds significant practical importance in guiding production. It not only reduces reliance on labor but also enhances production interactivity, precision, and automation.

Constructing rational, universal, and unified models based on the structural form and deformation behavior of Weft Knitted Fabrics is a prerequisite for dynamic simulation. Modeling methods primarily fall into two categories: geometry-based and physics-based approaches.

Geometry-based methods delineate the structure and form of fabric's basic units using key points and lines, and then use combinations and arrangements of these basic units to construct models. The Pierce loop model uses cylindrical representation of legs to connect the Needle loop and sinker loop represented by semicircular rings, with a highly idealized structure (Peirce, 1947). Kurbağ and Alpyıldız (2008) divided the loop into different segments according to its different regions, with each segment having its corresponding function, and the segmented functions often being

quite complex to closely approximate the real geometric structure of the fabric. Jiang et al. (2017) proposed a loop model based on binding points and fitted the center line of the loop with Bezier curves. Xin et al. (2018) used NURBS curves and loop-type value points to establish the structural morphology of the knitted fabric by determining the node vector using the chord length parameterization method and then inverse calculating the control points to fit the curve. Physics-based methods describe the deformation behavior of fabrics mathematically and physically by studying their physical characteristics and analyzing changes in their structural morphology.

Physics-based methods, on the other hand, describe the fabric's deformation behavior using mathematical and physical means by studying its physical properties. For instance, Abghary et al. (2018) used the finite element method to numerically simulate the deformation behavior of knitted fabrics and obtained a highly consistent tensile stress-strain curve with experimental measurements. Sha et al. (2017) proposed a cuboid mass-spring model to simulate the deformation of fabrics based on the proportional relationship between stitch offset and loop parameters.

Structural models established using geometry-based methods often have limitations in that they are primarily applicable to uniformly regular fabrics. On the other hand, deformation models based on physics often describe stitchal changes but lack the representation of yarn morphology. Therefore, it is essential to study the relationship between structural models and deformation models and construct

associated models to support simulation and modeling efforts.

In this study, we focus on the basic stitch of weft knitted fabrics and establish three-dimensional structure models and improved mass-spring deformation models based on binding points. Subsequently, we construct a correlation model between the structure model and the deformation model using binding points as the link and use NURBS curve application, force analysis, dynamics solution and other methods to design and present the correlation model. Finally, we implement the dynamic simulation of structural deformation of weft knitted fabrics using Code::Blocks, C++, and OpenGL.

2. Three-dimensional structure model

The basic stitch of weft knitted fabrics is divided into plain stitch, rib stitch and purl stitch according to the different arrangement of the front and back side of the loops (Cherif et al., 2012).

2.1. Modeling

The geometric structure of loop units is symmetrical to the left and right (Deng Jie & Jun-Zei, 2011), and its left half is symmetric about the center. A three-dimensional structure model of loop units based on binding points is established as shown in Figure 1. Binding points are set at the interlocking positions of loops to locate the loop units (Jiang et al., 2017), while type value points on the centerline of the loop, represented by dashed lines, define the spatial shape of the loop. The positions of binding points are shown by star P and pentagon O in the figure, representing the interlocking positions between the loop and the corresponding loops above and below (Liang Jialu, 2020). The positions of type value points are shown by triangular points in the figure: T_4 represents the highest point of the needle loop, T_3 and T_5 represent the connection between the needle loop and the legs, T_1 and T_7 represent the connection between the sinker

loop and the legs, T_0 and T_8 represent the connection between the loop and the loops on the left and right sides, i.e. the lowest point of the sinker loop, and T_2 and T_6 represent the symmetrical points of the left and right legs, which are also the most protruding points of the legs.

The plain stitch is formed by continuous interlocking of loops in one direction. Making reasonable assumptions and simplifications regarding the physical object, it is assumed that there is no compression deformation or stretching deformation between loops when the plain stitch is statically placed, and between the loop for uniform regular fit connected (Lu et al., 2016). The three-dimensional structure model of the plain stitch is established as shown in Figure 2. The yarn radius is denoted as r . The thickness of the loop unit, M , is reflected by 2 yarn diameters and the loop gap equivalent to 1 yarn radius, i.e. $5r$. The width of the loop unit, D , is reflected by the width of the needle loop formed by 4 yarn diameters, i.e. $8r$. The height of the loop unit, H , is a combination of the heights of the needle loop formed by 2 yarn diameters, the heights of the sinker loop formed by 2 yarn diameters, and the height of the legs. The height of the legs is equal to the distance between the binding points above and below, which includes the height of the sinker loop of the previous row of loops and the height of the needle loop of the next row of loops. Due to the overlap of 1 yarn radius between the binding points, the vertical distance between the binding points can be calculated as $3r + r + 3r$, resulting in a loop height of $4r + 3r + r + 3r + 4r$, i.e. $15r$.

The rib stitch and purl stitch woven by two needle beds have twice the thickness of the plain stitch woven by one needle bed (Lu & Jiang, 2017). However, without considering the shrinkage deformation, the width and height of the stitch remain unchanged (Asayesh & Amini, 2021). The three-dimensional structure models of the 1+1 rib stitch and 1+1 purl stitch before deformation are shown in Figures 3 and 4, respectively, with green indicating the front-side loops and blue indicating the back-side loops.

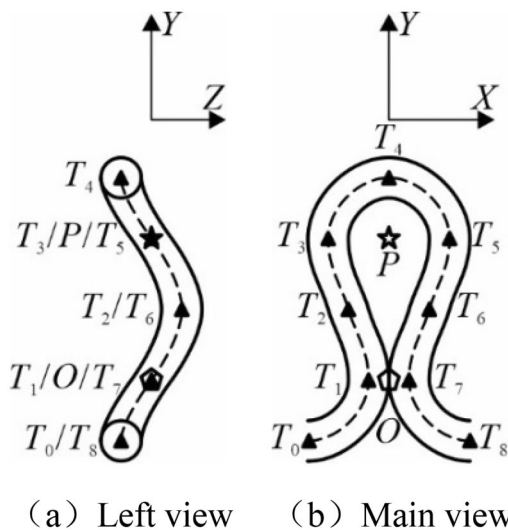


Figure 1. Three-dimensional structure model of loop unit.

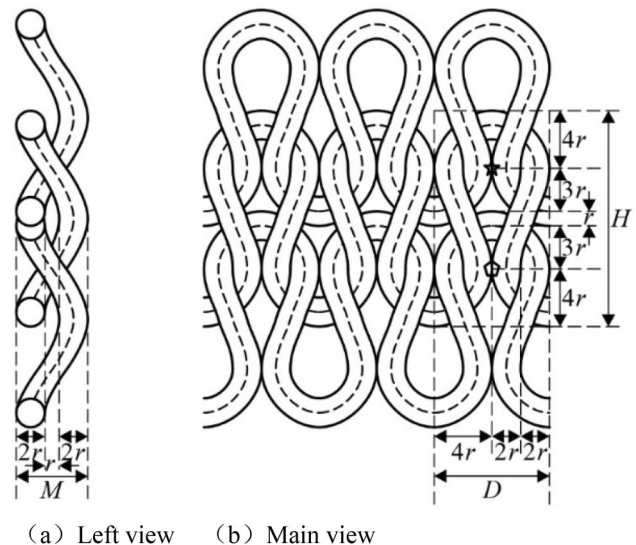


Figure 2. Three-dimensional structure model of the plain stitch.

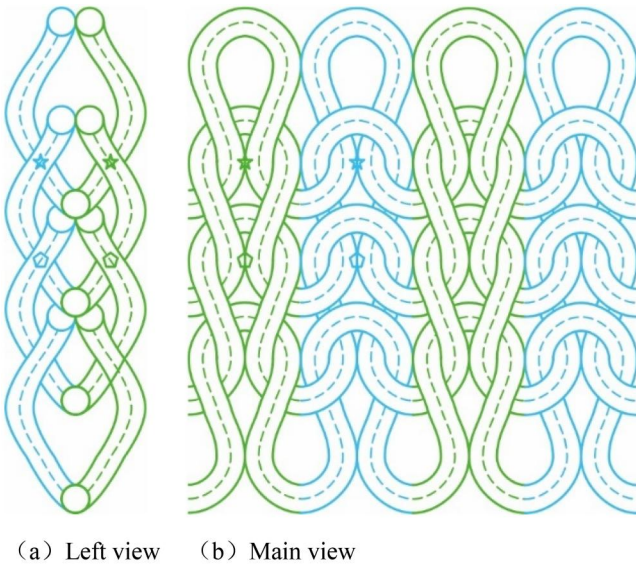


Figure 3. Three-dimensional structure model of the 1 + 1 rib stitch.

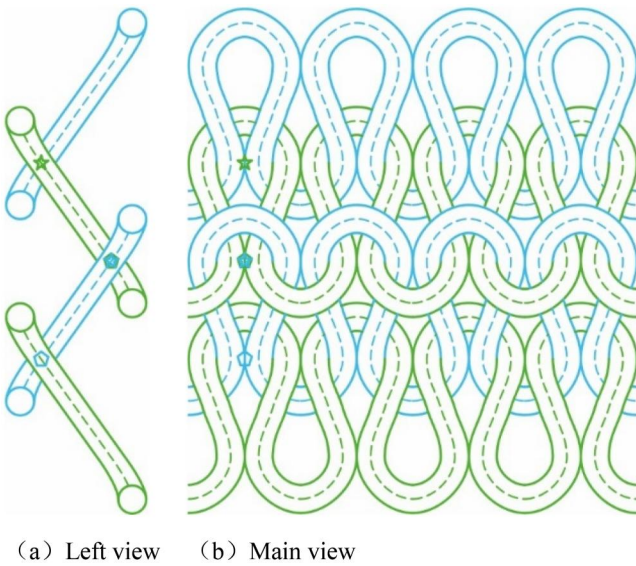


Figure 4. Three-dimensional structure model of the 1 + 1 purl stitch.

2.2. Data analysis

Let O_{ij} represent the lower binding point of the loop unit in the i -th row and j -th column of the plain stitch, and let P_{ij} represent the upper binding point. The type value points are denoted as T_{ij0} , T_{ij1} , ..., T_{ij7} , and T_{ij8} . Assuming the three-dimensional coordinates of O_{ij} are (x, y, z) , because the X and Z coordinates of P_{ij} are the same as those of O_{ij} , and the height between the upper and lower binding points of the same loop unit is $3r + r + 3r$, the three-dimensional coordinates of P_{ij} are $(x, y + 7r, z)$. Since the lower binding point $O_{i(j-1)}$ of the left adjacent loop unit has the same Y and Z coordinates as O_{ij} , and the width between the two lower binding points is the width of one loop unit, i.e. $8r$, the three-dimensional coordinates of $O_{i(j-1)}$ are $(x-8r, y, z)$. Essentially, the upper binding point $P_{(i-1)j}$ of the loop unit below this loop unit has the same position as O_{ij} , so the three-dimensional coordinates of $P_{(i-1)j}$ are (x, y, z) . Similarly, the coordinates of binding points in other loop

units of the plain stitch can be obtained, as shown in Table 1.

By analyzing the positional relationships and coordinate representations of the binding points in the plain stitch, the mathematical relationship between their three-dimensional coordinates can be derived:

$$\begin{cases} P_{ij}.x = O_{ij}.x \\ P_{ij}.y = O_{ij}.y + 7r \\ P_{ij}.z = O_{ij}.z \end{cases} \quad (1)$$

$$\begin{cases} O_{(i+m)(j+n)}.x = O_{ij}.x + 8nr \\ O_{(i+m)(j+n)}.y = O_{ij}.y + 7mr \\ O_{(i+m)(j+n)}.z = O_{ij}.z \end{cases} \quad (2)$$

In Equation (2), m and n are integers.

By analyzing the structural relationships between type value points and binding points, it can be observed that T_{ij4} , T_{ij3} , and T_{ij5} are mainly controlled by the upper binding point; T_{ij2} and T_{ij6} are mainly controlled by both the upper and lower binding points; T_{ij1} and T_{ij7} are mainly controlled by the lower binding point; T_{ij0} is mainly controlled by the two lower binding points of the current loop and the left adjacent loop, and T_{ij8} is mainly controlled by the two lower binding points of the current loop and the right adjacent loop. Essentially, the type value point T_{ij0} of the loop unit is the same as the type value point $T_{i(j-1)8}$ of the left adjacent loop unit. Combining this information with Table 1, the corresponding coordinates of type value points in each loop unit can be obtained. For example, the coordinates of type value points in the i -th row and j -th column loop unit are shown in Table 2.

Based on the above analysis, partial mathematical relationships between type value points and binding points in the plain stitch can be established:

$$\begin{cases} T_{ij2}.x = (P_{ij}.x + O_{ij}.x)/2 - 2r \\ T_{ij2}.y = (P_{ij}.y + O_{ij}.y)/2 \\ T_{ij2}.z = (P_{ij}.z + O_{ij}.z)/2 + 1.5r \end{cases} \quad (3)$$

$$\begin{cases} T_{ij1}.x = O_{ij}.x - r \\ T_{ij1}.y = O_{ij}.y \\ T_{ij1}.z = O_{ij}.z \end{cases} \quad (4)$$

$$\begin{cases} T_{ij0}.x = (O_{ij}.x + O_{i(j-1)}.x)/2 \\ T_{ij0}.y = (O_{ij}.y + O_{i(j-1)}.y)/2 - 3r \\ T_{ij0}.z = (O_{ij}.z + O_{i(j-1)}.z)/2 - 1.5r \end{cases} \quad (5)$$

By considering the symmetric patterns of loop unit three-dimensional structure models, the mathematical relationships between other type value points and binding points can be derived.

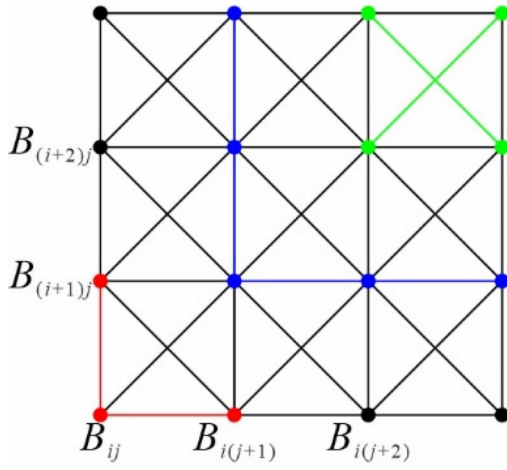
The rib stitch and purl stitch are derived from the plain stitch through certain regular adjustments. Therefore, based on the analysis and results of the plain stitch, and utilizing the principle of symmetry, the relationships between type value points and binding points in the corresponding stitch can be analyzed and established. These details are not elaborated here.

Table 1. Coordinates of some binding points in loop units.

Loop rows /columns	$j-1$ -th	j -th	$j+1$ -th
$i+1$ -th	$P_{(i+1)(j-1)}(x-8r, y+14r, z)$ $O_{(i+1)(j-1)}(x-8r, y+7r, z)$	$P_{(i+1)j}(x, y+14r, z)$ $O_{(i+1)j}(x, y+7r, z)$	$P_{(i+1)(j+1)}(x+8r, y+14r, z)$ $O_{(i+1)(j+1)}(x+8r, y+7r, z)$
i -th	$P_{i(j-1)}(x-8r, y+7r, z)$ $O_{i(j-1)}(x-8r, y, z)$	$P_{ij}(x, y+7r, z)$ $O_{ij}(x, y, z)$	$P_{i(j+1)}(x+8r, y+7r, z)$ $O_{i(j+1)}(x+8r, y, z)$
$i-1$ -th	$P_{(i-1)(j-1)}(x-8r, y, z)$ $O_{(i-1)(j-1)}(x-8r, y-7r, z)$	$P_{(i-1)j}(x, y, z)$ $O_{(i-1)j}(x, y-7r, z)$	$P_{(i-1)(j+1)}(x+8r, y, z)$ $O_{(i-1)(j+1)}(x+8r, y-7r, z)$

Table 2. Coordinates of type value points in a specific loop unit.

Type value points	Three-dimensional coordinates	Type value points	Three-dimensional coordinates	Type value points	Three-dimensional coordinates
T_{ij2}	$(x-2r, y+3.5r, z+1.5r)$	T_{ij3}	$(x-3r, y+7r, z)$	T_{ij6}	$(x+2r, y+3.5r, z+1.5r)$
T_{ij1}	$(x-r, y, z)$	T_{ij4}	$(x, y+10r, z-1.5r)$	T_{ij7}	$(x+r, y, z)$
T_{ij0}	$(x-4r, y-3r, z-1.5r)$	T_{ij5}	$(x+3r, y+7r, z)$	T_{ij8}	$(x+4r, y-3r, z-1.5r)$

**Figure 5.** Traditional mass-spring model.

3. Mass-spring deformation model

Weft knitted fabrics have excellent extensibility and elasticity in both transverse and longitudinal directions, which means that their structures are easily subjected to forces and undergo deformation.

3.1. Traditional model

The mass-spring model assumes that the ordered loops in knitted fabrics are points with mass, i.e. mass points. The mass points are connected by springs to represent the interactions between the loops (Deng Yifei & Wei, 2018). The traditional mass-spring model, as shown in Figure 5, represents mass points as dots and springs as straight lines. The springs can be classified into three types: structural springs, shear springs, and bending springs, which control the forces in the warp and weft, oblique, and folded bending directions, respectively, as indicated by the red, green, and blue markers in the figure.

In the traditional mass-spring model, the mass positions are uniformly distributed, and the spring connections are fixed. This model is relatively regular and is often used for fabric flexibility simulation, especially for woven fabrics with warp and weft interlacing structures. To some extent, it can also describe the structural morphology of knitted fabrics. However, it has limitations in capturing the detailed

structural changes after deformation. The traditional model cannot fully match the actual fabric behavior.

3.2. Improved model

To address the limitations of the traditional mass-spring model in simulating knitted fabrics, an improved mass-spring model based on the binding points of loops is proposed. The regular model is transformed into an adjustable model, considering the characteristics of loop units. The improved mass-spring deformation model for loop units is illustrated in Figure 6. The basic unit is the loop unit, and the mass positions are set at the binding points. In between the lower binding points of adjacent loop units, the weft springs are established to represent the forces between loop units in the weft direction and the course direction of yarn, as shown by the horizontal lines and arrows in the figure. Warp springs are added between the upper and lower binding points within the same loop unit to represent the forces between loop units in the warp direction and the warp direction of yarn, as indicated by the vertical lines and arrows in the figure.

Based on the stitch structure of weft knitted fabrics, an improved mass-spring deformation model for plain stitch is established based on loop units, as shown in Figure 7, where a loop unit is enclosed by a dashed rectangle. Except for the edge loops, due to the interlocking relationship between loops, the upper binding point of a loop is typically positioned above the lower binding point of another loop, and both binding points follow the principle of positional unity, determining the position of the corresponding masses. In other words, each mass has at least one upper binding point and one lower binding point. The weft springs and warp springs between the binding points in the improved mass-spring deformation model are connected to masses located at those binding points. Essentially, they are equivalent to the structural springs between masses in the traditional model. Since this study does not consider fabric folding-induced loop bending and shear springs can be indirectly represented by the combined action of weft and warp springs, the bending springs and shear springs are omitted in the improved model.

By analyzing the geometric structure and positions of binding points in rib and purl stitch, corresponding

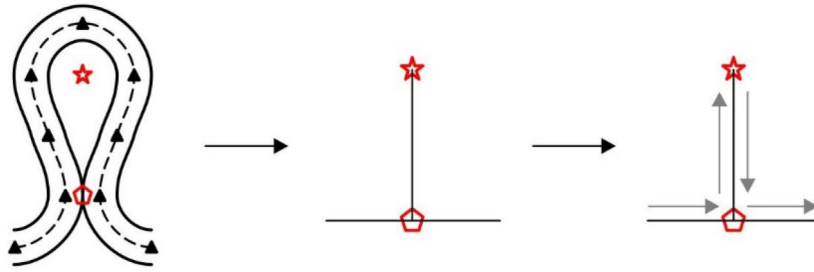


Figure 6. Improved mass-spring deformation model for loop units.

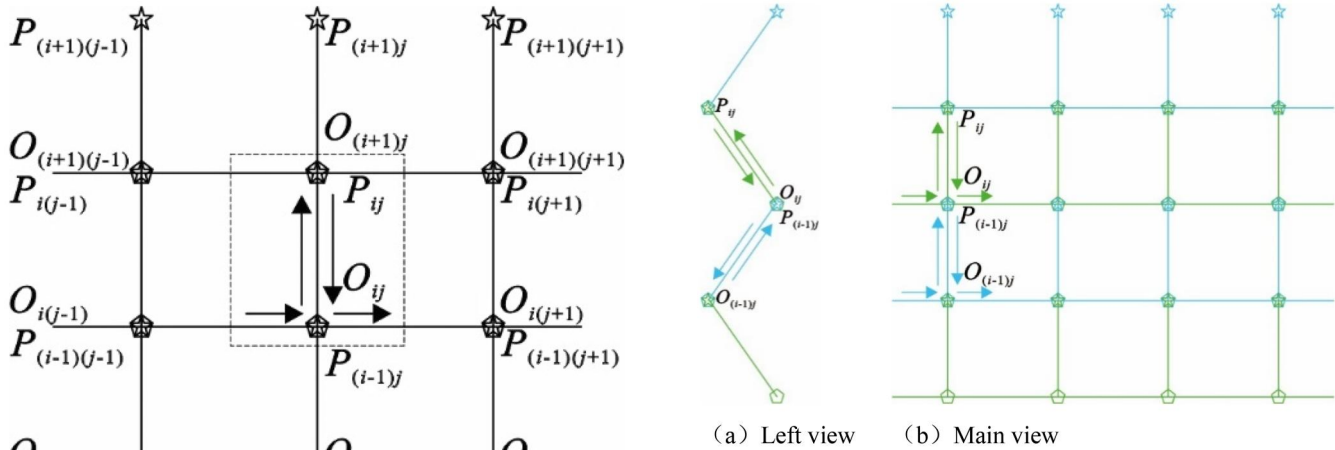


Figure 7. Improved mass-spring deformation model for plain stitch.

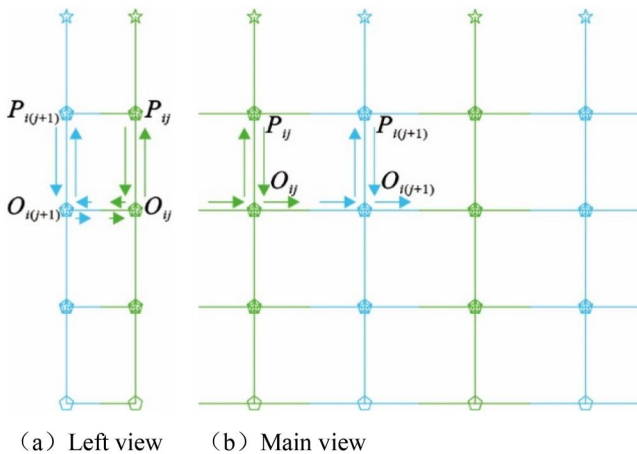


Figure 8. Improved mass-spring model for 1 + 1 rib stitch.

improved mass-spring deformation models before the deformation behavior of these stitches can be established, as shown in Figures 8 and 9. In accordance with the three-dimensional structural models, the green color represents the front loops, and the blue color represents the back loops. In the rib stitch, the weft springs between the lower binding points of adjacent loops are displayed with a certain width in the left view. In the purl stitch, the warp springs between the upper and lower binding points within each front and back loop are displayed with a certain inclined width in the left view.

Figure 9. Improved mass-spring model for 1 + 1 purl stitch.

3.3. Summary

Based on loop units and binding points, traditional models have been improved by transforming them into adjustable models. This modification retains the advantages of traditional models while making the improved model align better with the stichal structure of weft knitted fabrics. In the improved model, the warp-wise springs and weft-wise springs individually control the forces and movements in the left-right and up-down directions of the loop units. Simultaneously, the forces and movements of the loop units in other directions are influenced by the combined action of the warp-wise and weft-wise springs, enabling the loop units to experience forces and movements in all directions. Furthermore, the improved model can adapt the states and positions of intersections and springs based on changes in loop unit types and variations in fabric stichal forms. This results in improved mass-spring models for various stichal structures within weft knitted fabrics, serving as the foundation for dynamic simulations of a diverse range of fabric types.

4. Correlation model construction and simulation

Currently, there are numerous modeling methods and diverse model types for weft knitted fabrics. However, most deformation models are separate from structural models, resulting in a significant increase in model complexity, redundant data, and fragmented implementations. Therefore, it is necessary to explore the connection between

structural models and deformation models to obtain a correlation model that integrates the advantages of both.

4.1. Associated structural model and deformation model

As the foundation and central element of both the structural and deformation models, binding points serve as the link between the two. By focusing on the binding points, three-dimensional structural models are established based on the data of loop-type value points in the fabric. An improved mass-spring deformation model is then created by placing and connecting loop masses and springs. This allows for the development of a correlation model consisting of two sub-modules: the structural model and the deformation model, as shown in Figure 10.

When the state and position of a binding point change due to alterations in the fabric structure or other factors, the corresponding mass's state and position also change. The connected springs undergo deformation, resulting in the application of forces. The masses experience velocity and acceleration due to the forces acting upon them. To ensure system energy conservation and stabilization, the masses and springs undergo dynamic changes. The binding points, which follow the principle of positional unity with the masses, experience displacement. The type value points, which are geometrically related to the binding points, also undergo dynamic changes, leading to the dynamic deformation process of the loop's centerline.

4.2. NURBS curve application

NURBS curves have a unified representation form and the advantage of changing any control point without affecting the shape structure of other curve segments. They are convenient to compute and provide flexibility in control. In 1991, the International Stitch for Standardization (ISO) incorporated NURBS as the sole mathematical method for defining the geometric shape of industrial products in the industrial product data exchange standard STEP. NURBS is a modeling technique specifically tailored for curves and

surfaces, allowing for the creation of various intricate designs and the representation of distinctive effects, such as human skin, facial features, or streamlined automobiles.

They are computationally efficient and offer flexible control. In practical applications, NURBS curves can be categorized into two situations: forward calculation problems, where the curve's type value points are known, and the control points are determined to generate the curve, and inverse calculation problems, where the control points are unknown, and they need to be solved to fit the curve through known type value points.

Based on the three-dimensional structural model, the functional relationship between type value points and binding points can be obtained. Therefore, the position of the corresponding type value points can be calculated based on the state and position of the binding points. Then, using the principles of inverse calculation for NURBS curves, the control points of the curve can be determined from the type value points on the centerline of each row of loops. Finally, the control points are used to fit a NURBS curve to simulate the loop's centerline.

4.3. Force analysis

The deformation behavior of weft knitted fabrics is mainly caused by the interlocking and pulling of individual loop units. Therefore, a stress analysis of the fabric is conducted without considering external forces such as gravity and wind.

The forces acting on the masses mainly include the spring force F_s and the damping force F_d .

The spring force can be obtained using Hooke's law:

$$F_s = -K_s \Delta X \quad (6)$$

where K_s represents the spring's elastic coefficient, and ΔX represents the difference between the current length and the original length of the spring, which is the spring deformation vector. In this study, it is equivalent to the vector change in distance between the two mass positions (i.e. binding points) connected by the spring.

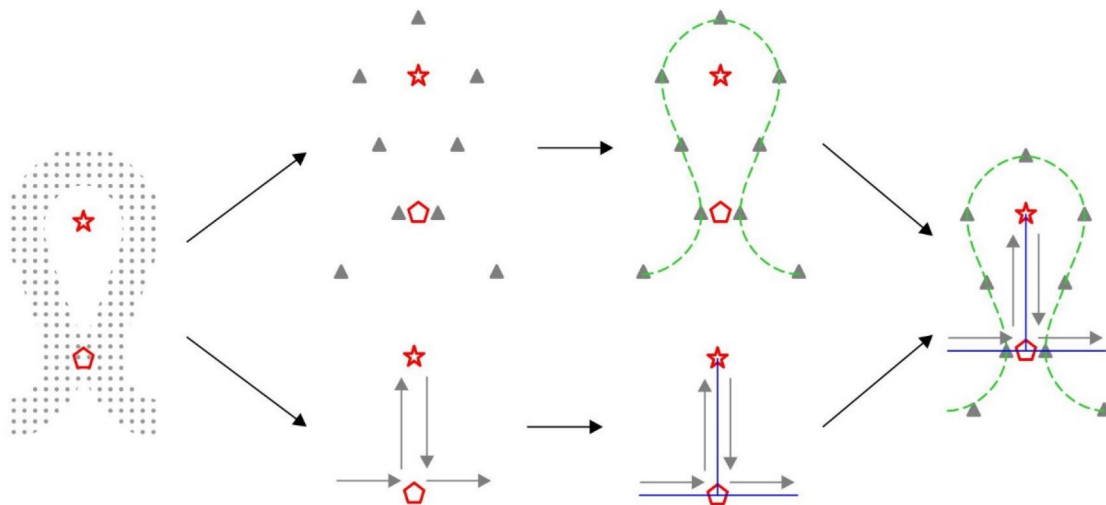


Figure 10. Model association steps.

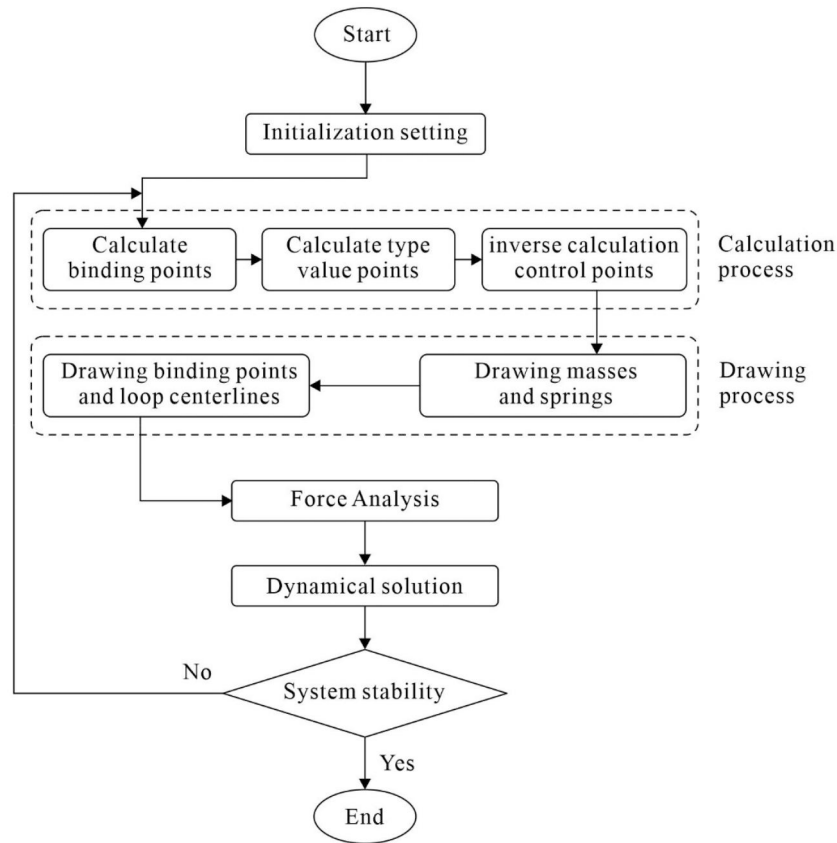


Figure 11. Program flow for simulated the correlation model.

The damping force is defined as:

$$F_d = -K_d \cdot V \quad (7)$$

where K_d represents the damping coefficient, and V represents the velocity vector of the mass.

Linking the force and acceleration of a mass according to Newton's second law:

$$F = F_s + F_d = m \cdot a \quad (8)$$

where m is the mass of the mass point, which can be determined by allocating the total mass of the knitted fabric to the binding points, and a is the acceleration of the mass point.

4.4. Dynamic solution

To solve the dynamic equations, commonly used methods include the Euler method and the Verlet integration method. The Euler method includes explicit Euler, implicit Euler, and semi-implicit Euler methods (Cuilian et al., 2022). Although the Euler method is easy to implement, it has drawbacks such as small computational volume, large errors, and instability. On the other hand, the Verlet integration method has significant advantages in terms of computational time step and accuracy. Therefore, this study adopts the Verlet integration method for research and application.

The expression for the Verlet integration method is as follows:

$$\begin{cases} X(t + \Delta t) = X(t) + V(t) \cdot \Delta t + \frac{1}{2} a(t) \cdot \Delta t^2 \\ V(t + \Delta t) = V(t) + \frac{1}{2} (a(t) + a(t + \Delta t)) \cdot \Delta t \end{cases} \quad (9)$$

where $X(t)$, $V(t)$, and $a(t)$ represent the position vector, velocity vector, and acceleration vector of the mass at time t , respectively, and Δt is the time interval.

5. Results and discussion

In order to dynamically simulate the structural deformation of the basic stitch of weft knitted fabrics, computer tools are employed for implementation. In the experimental environment with Windows 10 64-bit operating system, AMD Ryzen 7 5800H with Radeon Graphics 3.20 GHz CPU, 16GB memory, and a display resolution of 2560×1600 , the program flow for simulating the correlation model using the Code::Blocks integrated development environment, C++ language, and OpenGL function library is illustrated in Figure 11. Initially, the relevant data for two sub-modules, the three-dimensional structural model and the improved mass-spring deformation model, are configured through initialization. Subsequently, the states and positions of binding points are calculated based on the provided data, leading to the determination of type value points and control points through the reverse calculation method employing NURBS curves. Following this, masses and springs within the improved mass-spring deformation model, as well as

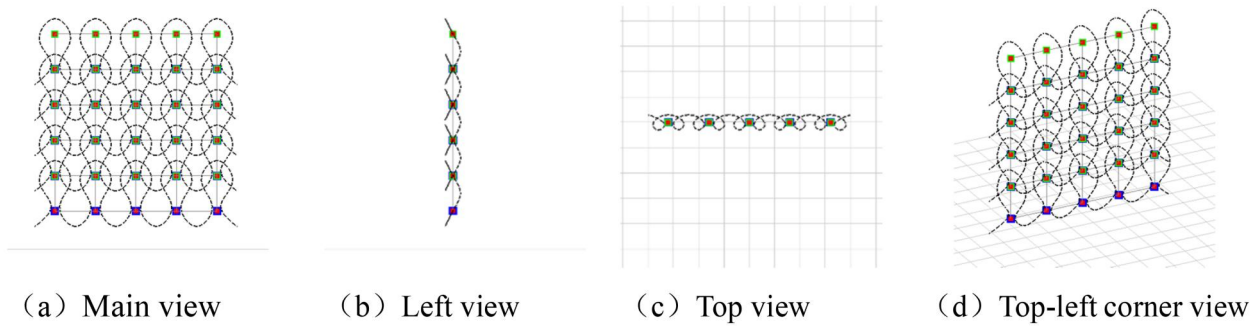
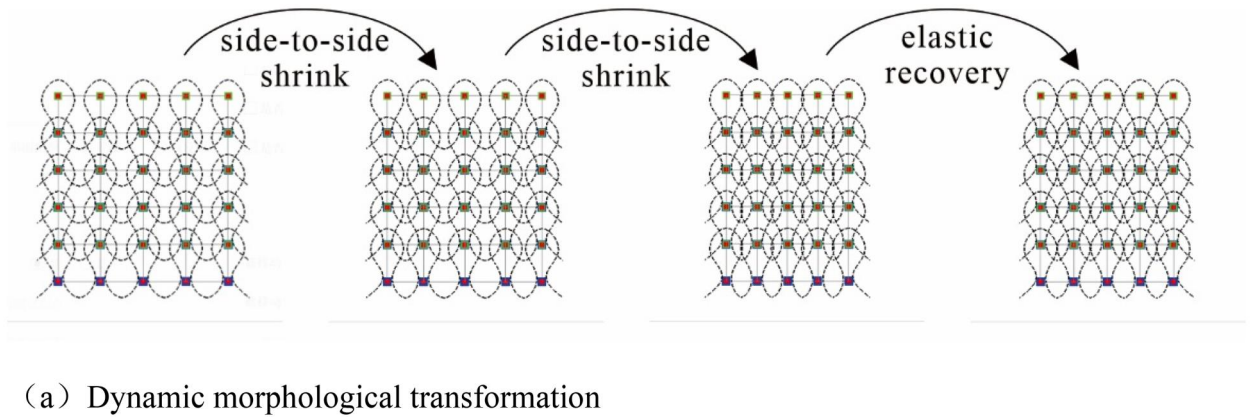


Figure 12. Plain stitch simulation.



(a) Dynamic morphological transformation

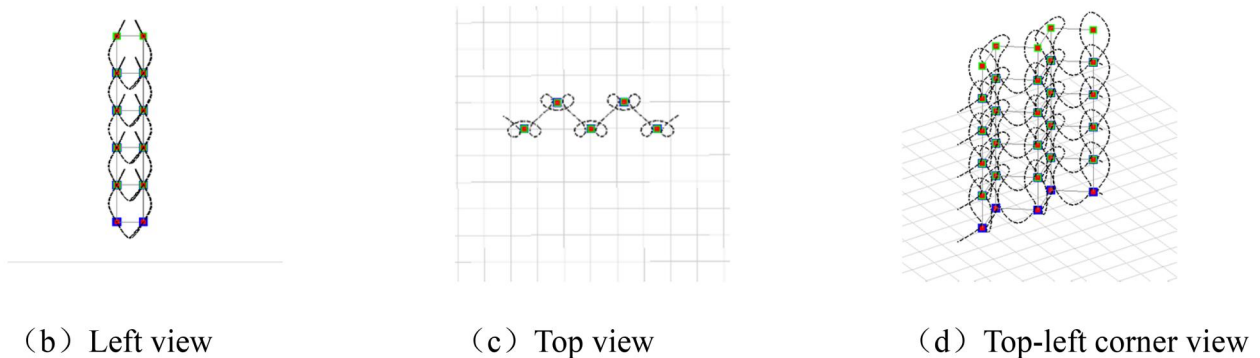


Figure 13. 1 + 1 Rib stitch simulation.

binding points and loop centerlines within the three-dimensional structural model, are rendered. The program continuously updates the positions of the points, which in turn updates the positions of the binding points, by calculating the forces and velocities of the points based on the force analysis and dynamic solutions outlined in '4.3. Force analysis' and '4.4. Dynamic solution' until the system reaches a stable state.

To make the spatial visualization of the simulation more obvious, a grid is drawn to simulate the floor as a spatial reference. The lower binding points are represented by blue cube points, the upper binding points are represented by green cube points, and the masses are represented by red cube points. Springs are represented by gray lines, and loop centerlines are represented by black dashed lines. Additionally, the simulation can be scaled, translated, and rotated using mouse operations.

The simulation of a plain stitch is shown in Figure 12. Figure 12(a–d) depicts the simulation results from different views, including the front, left, top, and top-left corner views, respectively, obtained through rotation operations.

The simulations of 1 + 1 rib stitch and 1 + 1 purl stitch structures are presented in Figures 13 and 14, respectively. In these figures, (a) illustrates the dynamic morphological transformation of the respective structures from their initial states to stable states. (b), (c), and (d) depict the simulated results from the left view, top view, and top-left corner view, respectively, after undergoing rotation operations.

From Figures 12–14, it can be inferred that by utilizing binding points to establish the correlation between the structural model and the deformation model, employing NURBS curves to simulate the loop centerline in the structural model, and conducting a rational analysis of the force distribution in the deformation model, the correlation

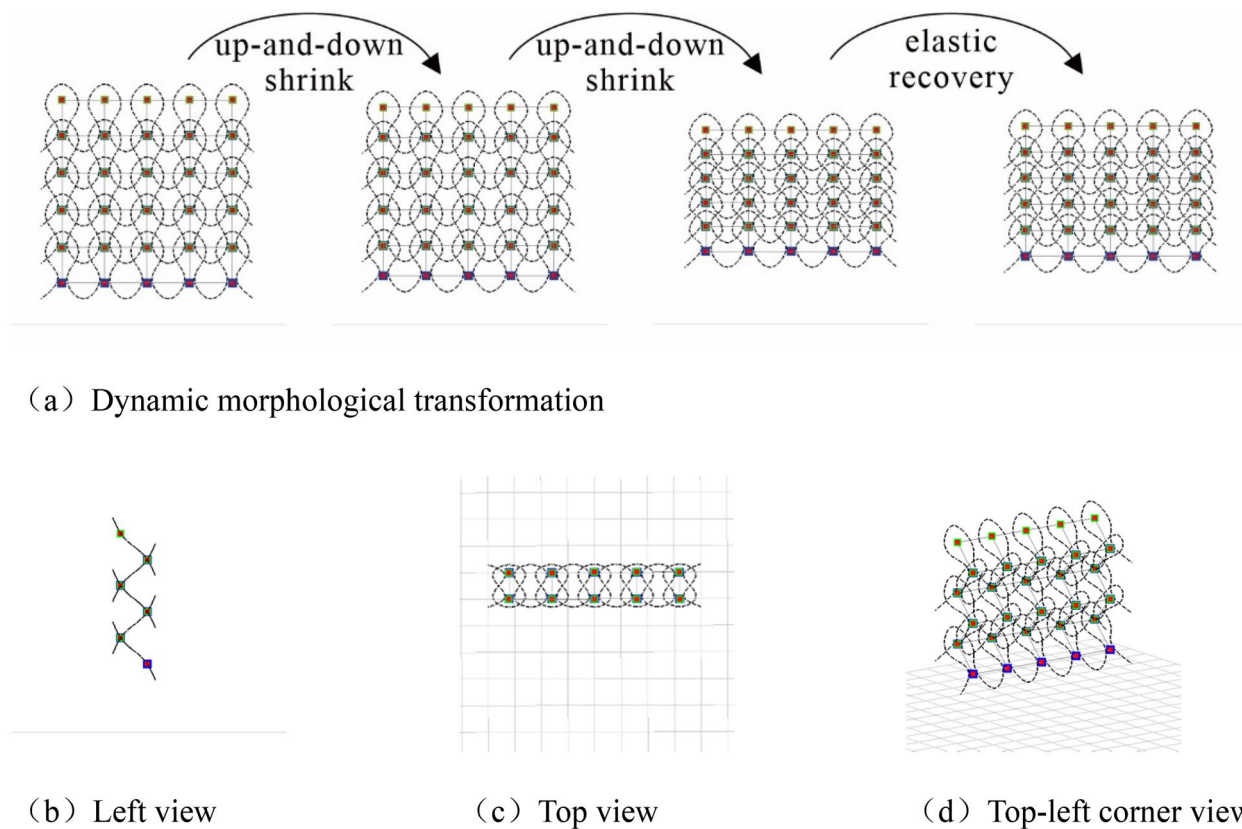


Figure 14. 1 + 1 Purl stitch simulation.

model can be continuously updated through dynamic solving. As a result, the dynamic deformation process of the basic structure of weft knitted fabrics can be effectively simulated. Additionally, this process serves as a reverse validation of the rationality and reliability of the three-dimensional structural model and the improved mass-spring deformation model.

Due to variations in the magnitude of forces acting on weft knitted fabrics under different conditions, this study lacks a quantification process for these forces. Subsequent research may involve parameterizing the forces exerted on the fabric, allowing for a more precise simulation of deformation processes under various scenarios.

6. Conclusion

By conducting in-depth research on the structural morphology and extension characteristics of fundamental stitches in weft knitted fabric, three-dimensional structural models and improved mass-spring deformation models were established based on binding points, encompassing plain stitch, rib stitch, and purl stitch. Data analysis was performed on the three-dimensional structural models. Subsequently, a correlation model between the structural model and the deformation model was constructed, with binding points serving as the link. The dynamic simulation of structural deformation in weft knitted fabric's basic stitch was achieved by applying the principle of NURBS curve inverse calculation to fit the loop centerline, analyzing force

distribution, solving dynamic equations, and utilizing computer technology.

Through the research content and findings presented in this paper, the aim is to achieve a visual and interactive three-dimensional dynamic simulation of weft knitted fabrics. This endeavor not only serves as a supportive tool for understanding knitted structures but also fosters the fabric design process and aids in predicting fabric production outcomes. Furthermore, it lays the foundation for the development of an integrated system for simulating, designing, and showcasing weft knitted fabrics.

Disclosure statement

No potential conflict of interest was reported by the author(s).

Funding

This work was supported by Research Project Supported by Shanxi Scholarship Council of China [2022-090].

References

- Abghary, M. J., Hasani, H., & Jafari Nedoushan, R. (2018). Prediction of deformation behavior of interlock knitted fabrics in different directions using FEM method. *The Journal of the Textile Institute*, 109(1), 1–7. <https://doi.org/10.1080/00405000.2017.1318690>
- Asayesh, A., & Amini, M. (2021). The effect of fabric structure on the compression behavior of weft-knitted spacer fabrics for cushioning applications. *The Journal of the Textile Institute*, 112(10), 1568–1579. <https://doi.org/10.1080/00405000.2020.1829330>

- Cherif, C., Krzywinski, S., Diestel, O., Schulz, C., Lin, H., Klug, P., & Trümper, W. (2012). Development of a process chain for the realization of multilayer weft knitted fabrics showing complex 2D/3D geometries for composite applications. *Textile Research Journal*, 82(12), 1195–1210. <https://doi.org/10.1177/0040517511429602>
- Cuilian, Y., Yan, C., & Hongyan, M. (2022). Stability of Euler methods for fuzzy differential equation. *Symmetry*, 14(6), 1279.
- de Araújo, M., Sousa Fangueiro, R. M. E., & Hong, H. (2004). Fibrous reinforcements for composite materials: Producing and modelling. *Materials Science Forum*, 455–456, 787–791. <https://doi.org/10.4028/www.scientific.net/MSF.455-456.787>
- Deng Jie, Q. C., & Jun-Zei, W. A. N. G. (2011). Dynamic simulation of knitted basic structure based on 3DS MAX. *SILK*, 8, 27–30.
- Deng Yifei, D. Z., & Wei, K. E. (2018). Stitch design and deformation simulation of cardigan based on loop model. *Journal of Textile Research*, 39(4), 151–157.
- Frydrych, I., Ahmad, Z., Wiener, J., Fraz, A., Siddique, H. F., & Havalka, A. (2018). Influence of weave design and yarn types on mechanical and surface properties of woven fabric. *Fibres & Textiles in Eastern Europe*, 26(1(127)), 42–45. <https://doi.org/10.5604/01.3001.0010.7795>
- Jiang, G., Lu, Z., Cong, H., Zhang, A., Dong, Z., & Jia, D. (2017). Flat knitting loop deformation simulation based on interlacing point model. *Autex Research Journal*, 17(4), 361–369. <https://doi.org/10.1515/aut-2016-0019>
- Kurbak, A., & Alpyildiz, T. (2008). A geometrical model for the double Lacoste knits. *Textile Research Journal*, 78(3), 232–247. <https://doi.org/10.1177/0040517507081306>
- Liang Jialu, C. H. (2020). Simulation structure model of weft-knitted two-side jacquard fabric. *SILK*, 57(11), 35–40.
- Lu, Z., & Jiang, G. (2017). Rapid simulation of flat knitting loops based on the yarn texture and loop geometrical model. *Autex Research Journal*, 17(2), 103–110. <https://doi.org/10.1515/aut-2016-0002>
- Lu, Z., Jiang, G., Cong, H., & Yang, X. (2016). The development of the flat-knitted shaped uppers based on ergonomics. *Autex Research Journal*, 16(2), 67–74. <https://doi.org/10.1515/aut-2015-0029>
- Peirce, F. T. (1947). Geometrical principles applicable to the design of functional fabrics. *Textile Research Journal*, 17(3), 123–147. <https://doi.org/10.1177/004051754701700301>
- Sha, S., Ma, P., Chapman, L. P., Jiang, G., & Zhang, A. (2017). Three-dimensional modeling and simulation of deformation behavior of fancy weft knitted stitch fabric. *Textile Research Journal*, 87(14), 1742–1751. <https://doi.org/10.1177/0040517516658518>
- Xin, R., Laihu, P., Minglai, L., Weimin, S., & Xudong, H. (2018). Modelling and algorithm of weft knitted fabric. *Journal of Textile Research*, 39(09), 44–49.